Low Density Nuclear Matter

Joseph B. Natowitz,
Department of Chemistry and Cyclotron Institute, Texas A&M University, College Station, Texas 77843, USA

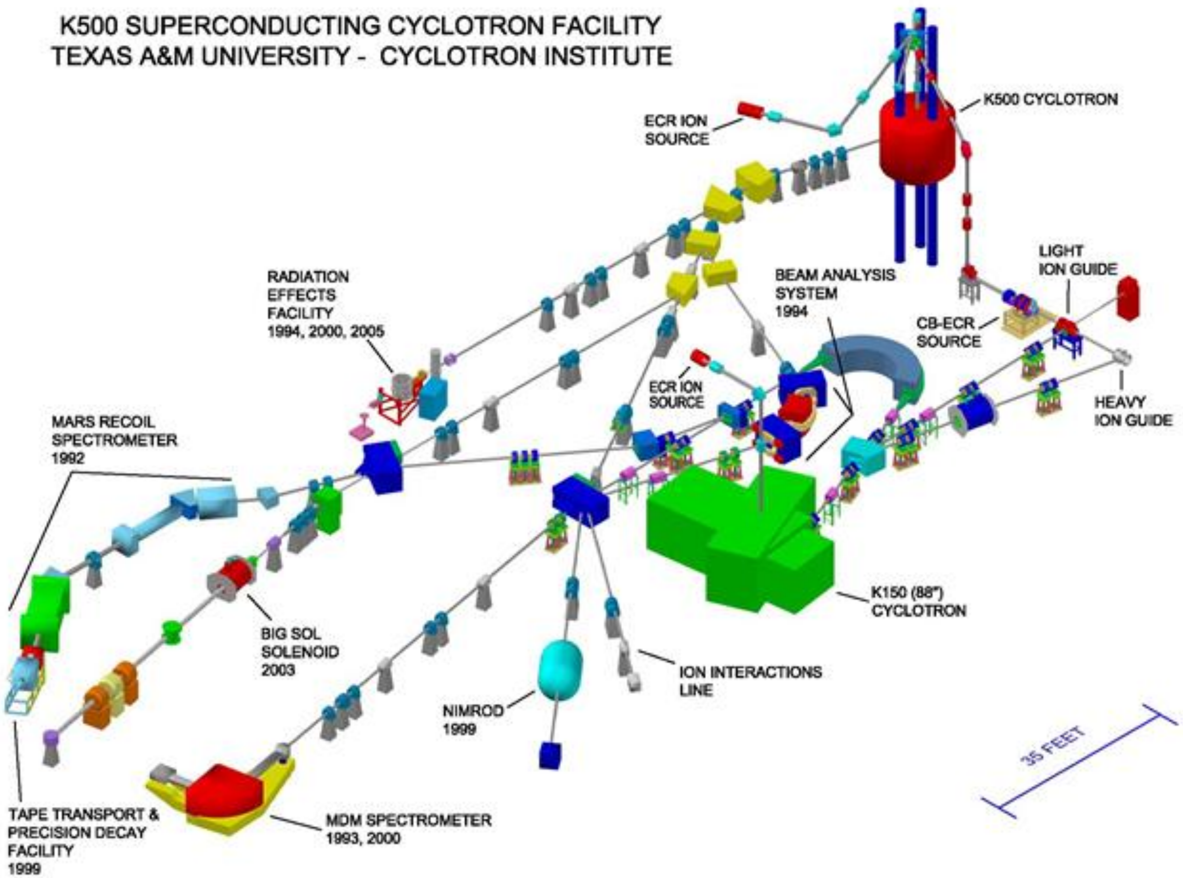

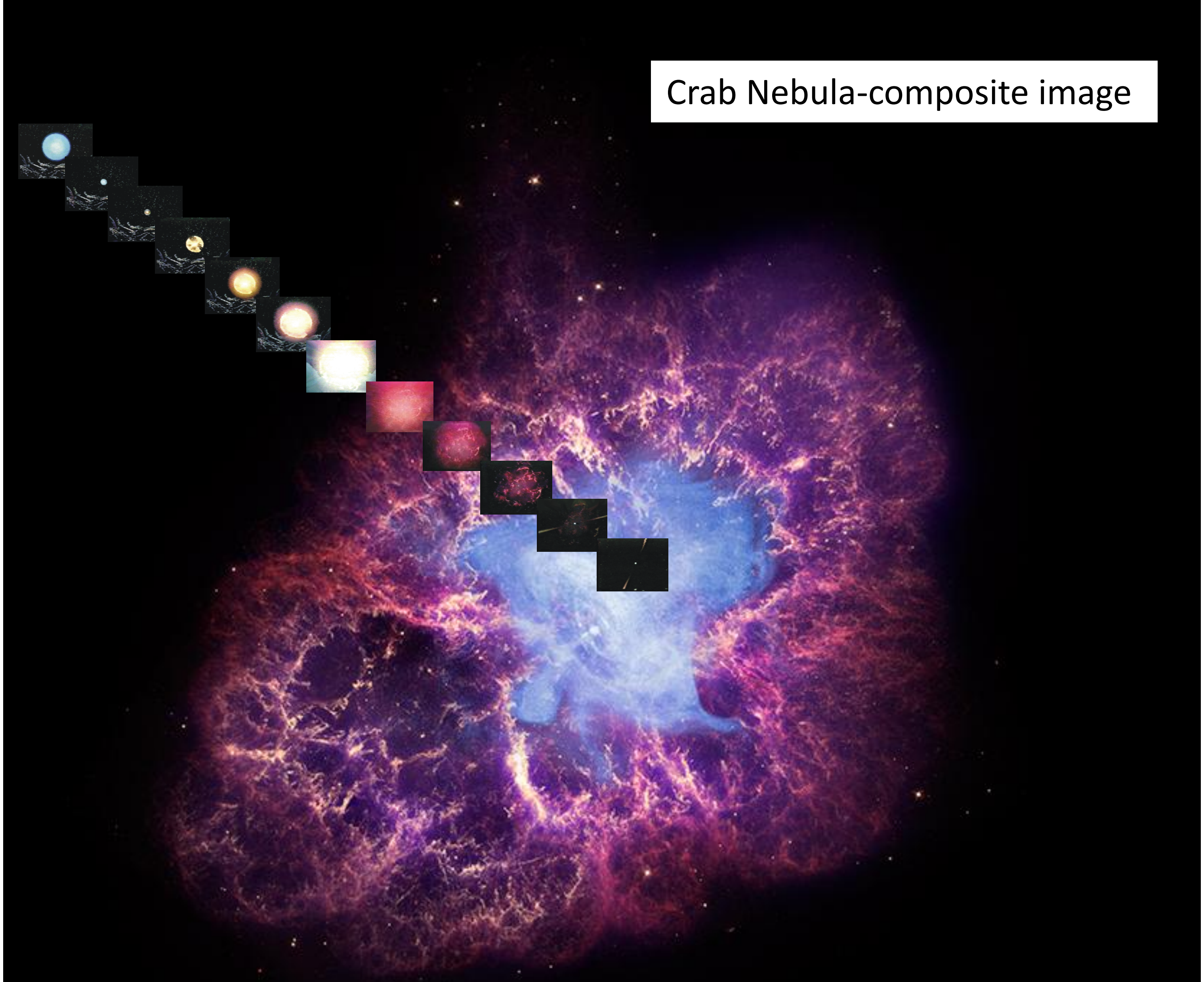

Explore the Nuclear and Astrophysical Equations of State –

Relevance of laboratory experiments to properties of the <u>Neutrino Surface</u>
in supernovae and binary mergers and nucleosynthesis in neutrino driven winds

- Core-collapse supernovae (SN)
  - Explosions of massive stars that radiate 99% of their energy in neutrinos
  - Birth places of neutron stars
  - Wide range of densities range from much lower than normal nuclear density to much higher
- Core Collapse Supernovae dynamics and the neutrino signals are sensitive to the details of neutrino interactions with nucleonic matter.
  - Neutrino properties determine the nucleosynthesis conditions in the so-called neutrino-driven wind
  - Detailed information on the composition and other thermodynamic properties of nucleonic matter are important to evaluate role of neutrino scattering.
- Details of neutrino heating depend both on matter properties of low density nuclear matter and the conditions at the neutrinosphere
  - Last scattering site of neutrinos in proto-neutron star: $\sim 10^{12}$ g/cm^3 ($\sim 6\times10^{-4}$ fm^{-3}), T~5 MeV
  - A thermal surface from which around 10^{53} ergs (10^{37} MeV) are emitted in all neutrino species during the explosion

The Neutrinosphere Problem

C.J. Horowitz, A. Schwenk   **nucl-th/0507033**

- View sun in neutrinos, see angular resolution of ν-e scattering in Super-K.
- View SN in neutrinos, see neutrinosphere. What does it look like?
- Conditions at neutrinosphere:
  - Temperature ~ 4 MeV crudely observed with 20 SN1987a events.
  - $\sigma \sim G_F^2 E_\nu^2$ and $E_\nu \sim 3T$
  - $\rho \sim 10^{11}$ g/cm^3 [$\sim 10^{-4}$ fm^{-3}]

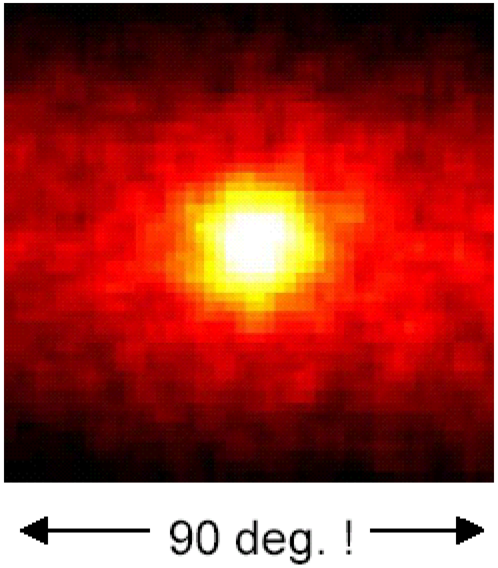

- What is the composition, EOS, and neutrino response of nuclear matter near the neutrinosphere?

Core-collapse supernovae

K.Sumiyoshi et al.,
Astrophys.J. **629**, 922 (2005)

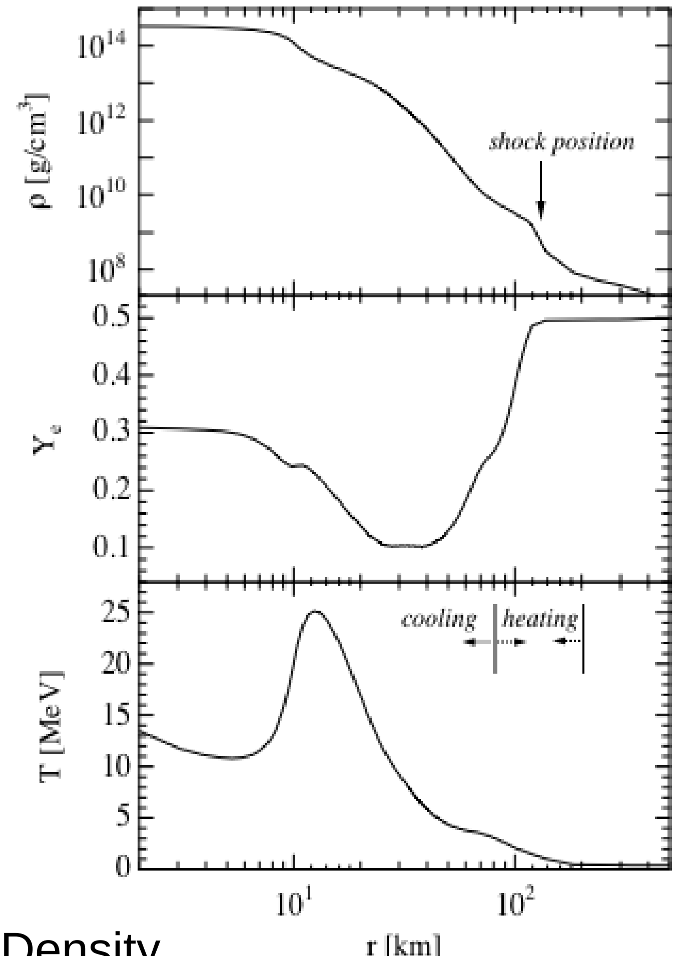

Density.
electron fraction, and
temperature profile
of a 15 solar mass supernova at 150 ms
after core bounce as function of the radius.

K.Sumiyoshi,
G. Roepke
PRC 77,
055804 (2008)

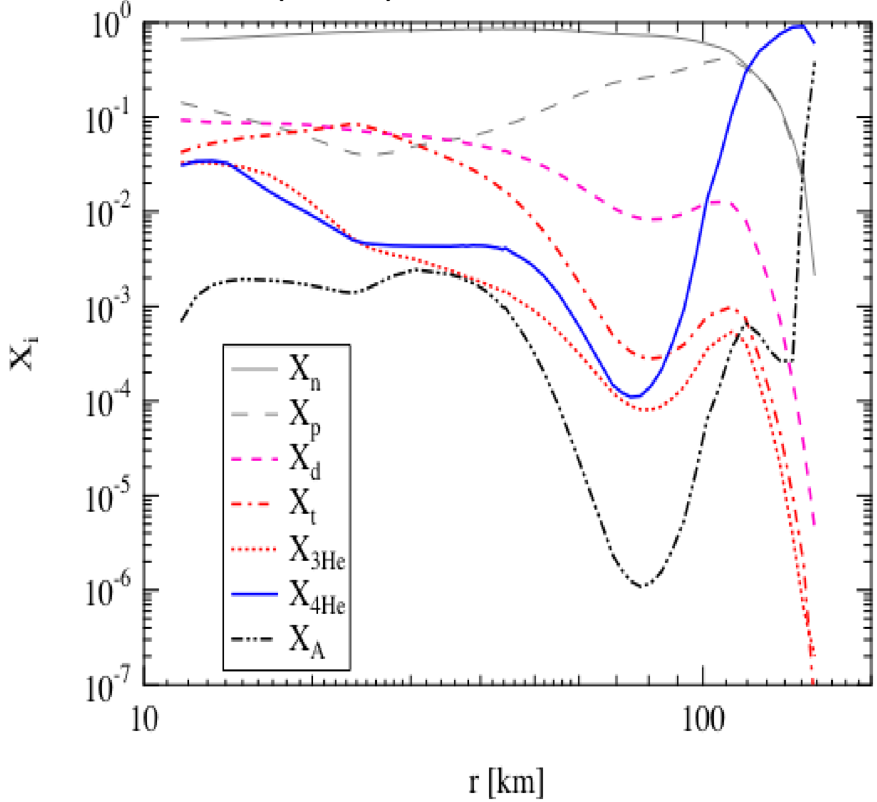

Mass fraction X of light clusters for a post-bounce supernova core

cluster formation Influences neutrino flux

- Relevance of heavy ion collisions to core collapse supernovae
  - Allow to probe the lower densities in the lab
  - Comparisons of heavy ion data to supernovae calculations may help discriminate between different models.
- Clusters appear in shock heated nuclear matter
  - Clusters Role on the explosion dynamics and the subsequent cooling and compression of the proto-neutron star is not yet fully understood
  - Valid treatment of the correlations and clusterization in low density matter is a vital ingredient of astrophysical models
- Equation of state (EOS)
  - Many fundamental connections between the equation of state and neutrino interactions
  - Crucial input for understanding proto-neutron star evolution

Exploring The Nuclear Matter Equation of State in the Laboratory With Collisional Heating

NEAR FERMI ENERGY HEAVY ION COLLISIONS AT LOW IMPACT PARAMETER

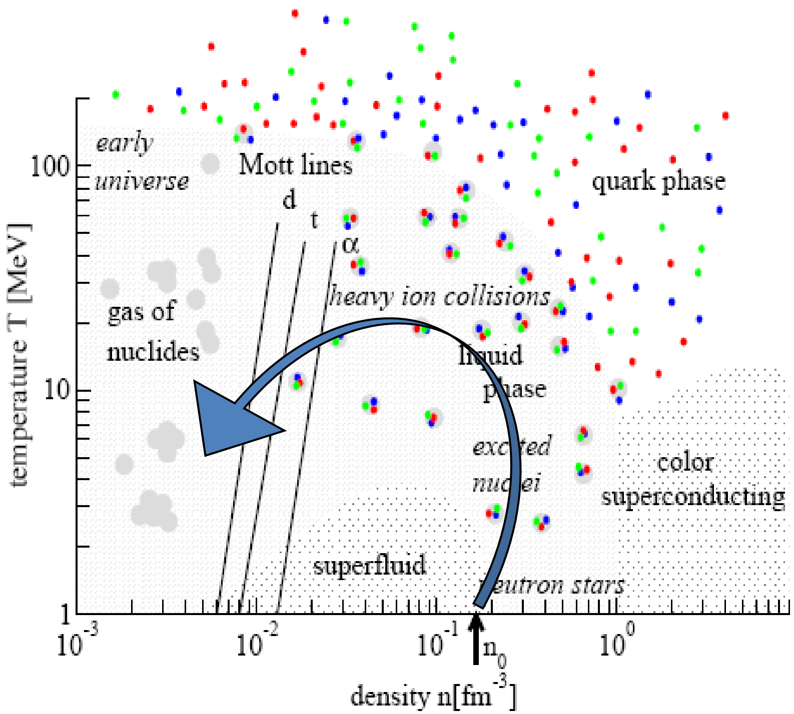

Figure 1. Schematic view of the phase diagram of nuclear matter. The phase
is empirical accessible by heavy ion collisions, excited nuclei, observation of neutron stars and the early universe as indicated in the diagram. New plans at GSI aim at exploring the color superconducting phase as well.

Time fm/c

0

50

100

200

300

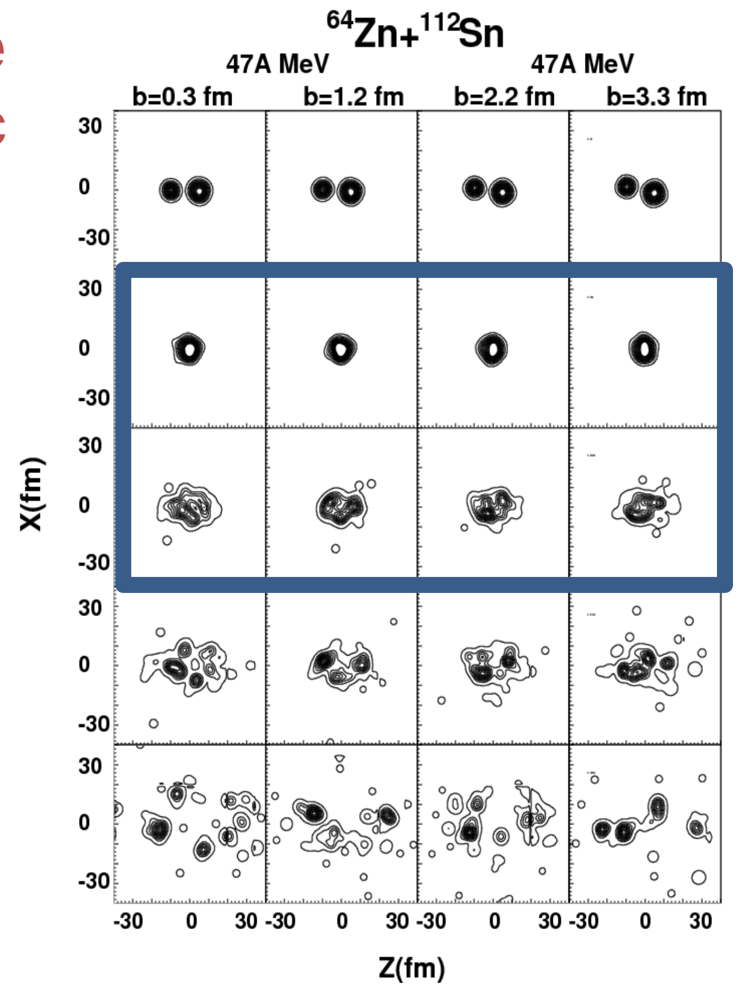

Antisymmetrized Molecular Dynamics Model* Calculations *A. Ono

Light Charged Particle Emission - Thesis – L. Qin TAMU

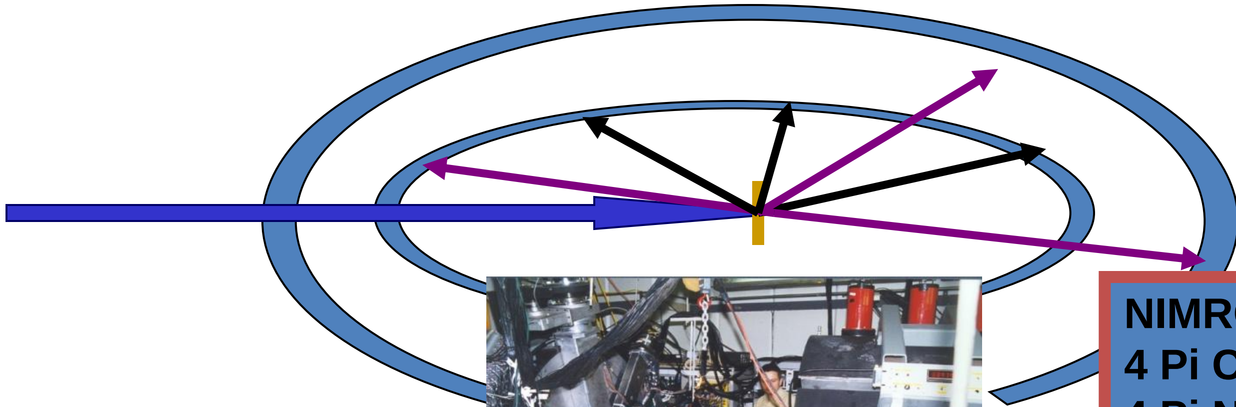

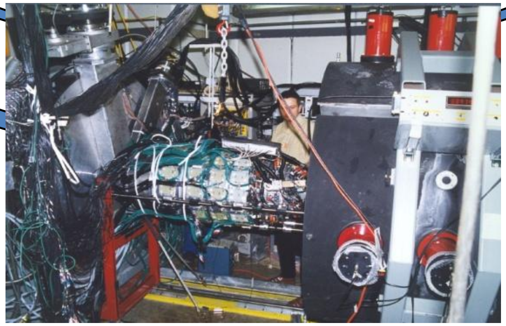

NIMROD
4 Pi Charged Particles
4 Pi Neutrons
Particle ID
Energy, Angle
Event by Event Correlations

Projectile Energy - 47A MeV

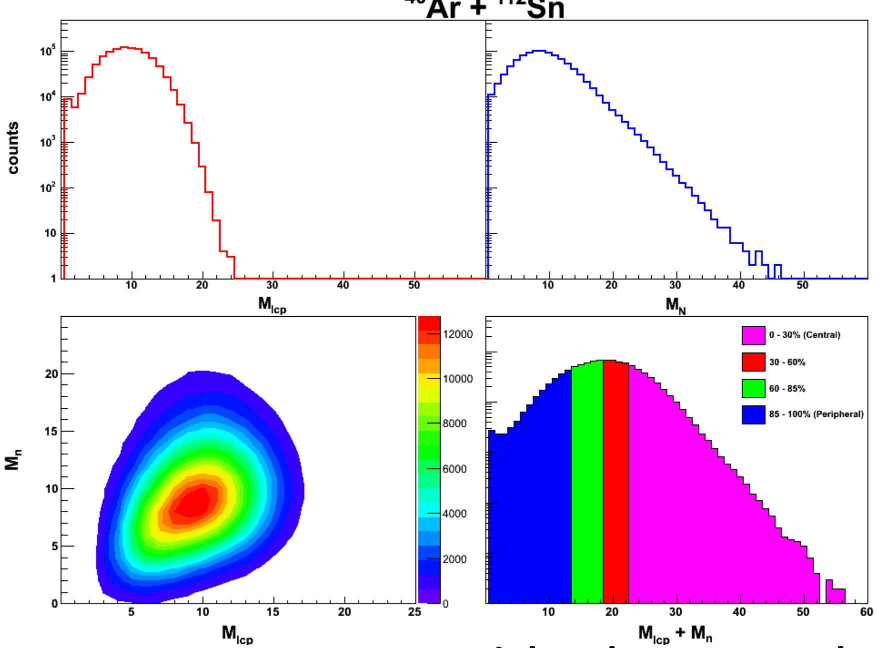

peripheral **central**

^{112}Sn ^{124}Sn

^{64}Zn
^{40}Ar
^{20}Ne
^{10}B
^{4}He

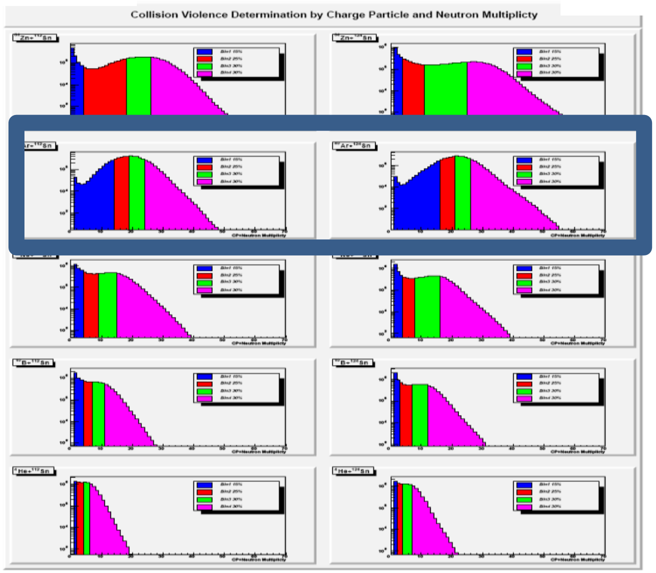

Fig. 34. Sum of neutron and charged particle multiplicty distribution of each reaction system. Bin4 corresponds to the most violent collision events, Bin3 corresponds to the semiviolent events, Bin2 corresponds to the semiperipheral events, and Bin1 corresponds to the peripheral events.

Light Charged Particle Emission - High Total Multiplicity Collisions

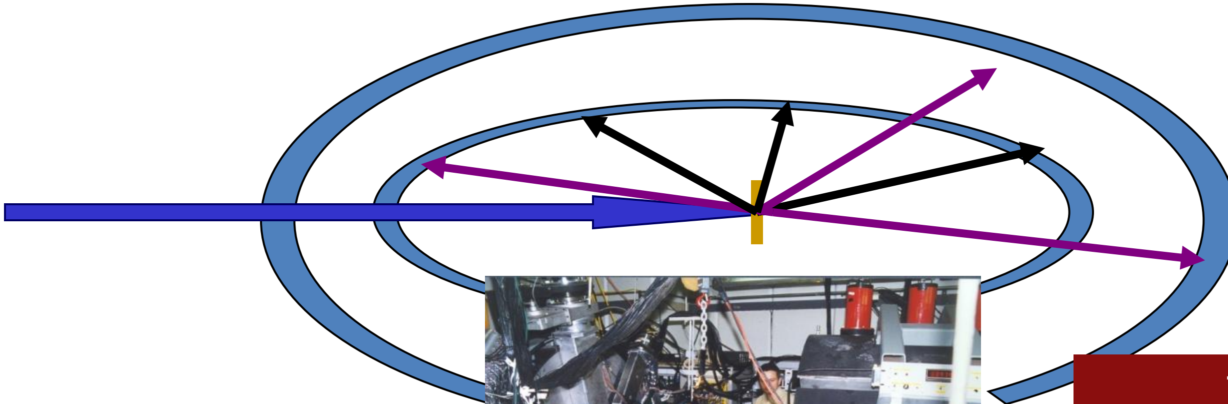

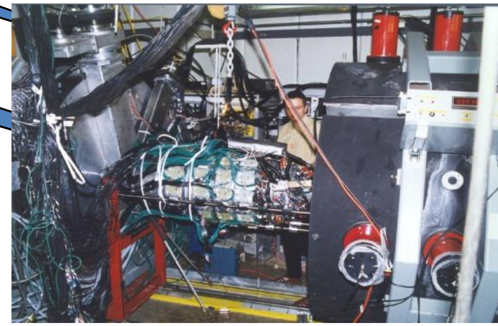

Projectile Energy - 47A MeV

Thesis – L. Qin
TAMU

Global Fits
3 Sources

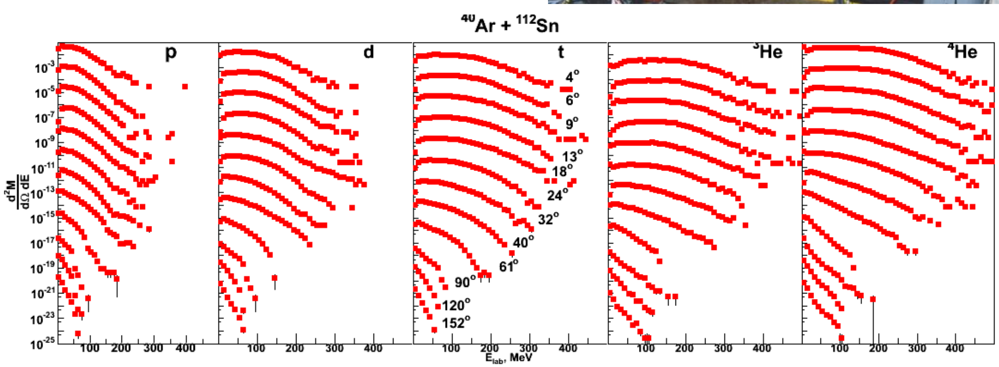

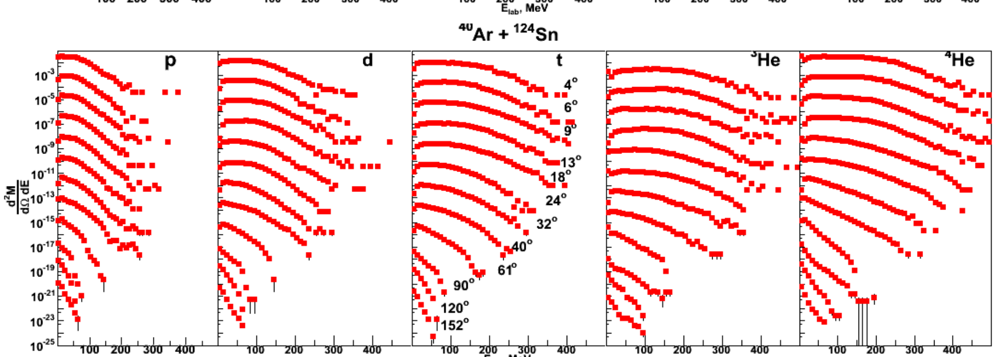

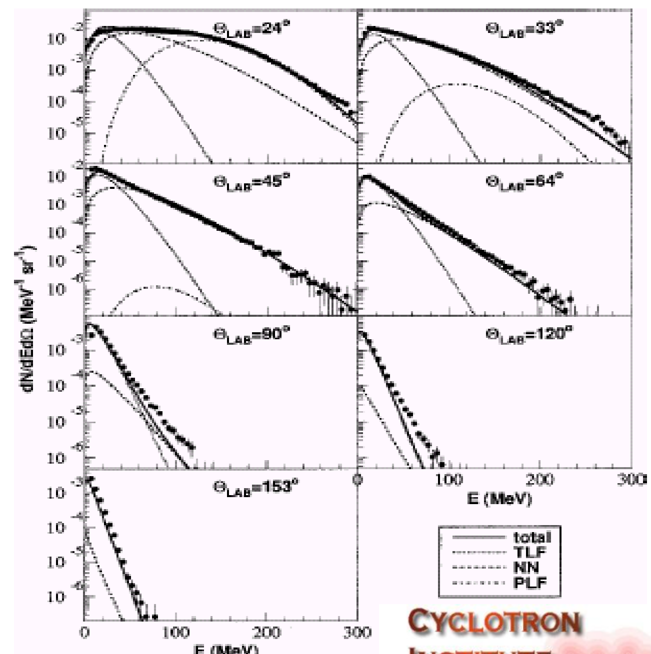

Velocity Plots- Light Charged Particles

From Fitting

Experiment

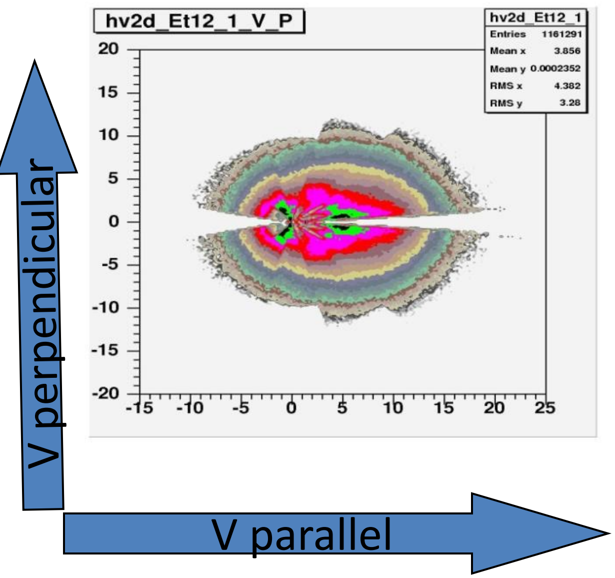

Velocity Plot Protons
$^{40}Ar+^{124}Sn$

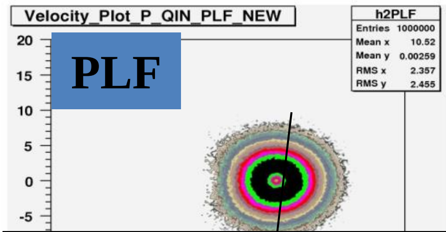

PLF

Sampling the GAS- early emission faster particles

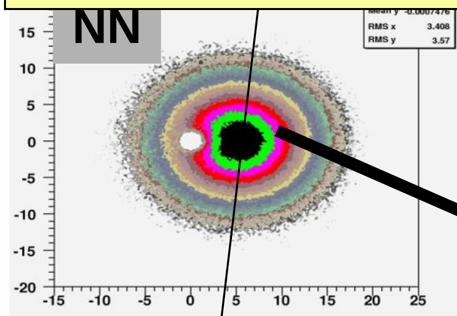

NN

Sum of Source Fits

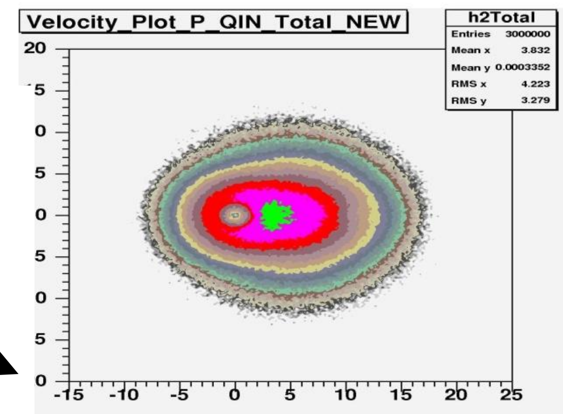

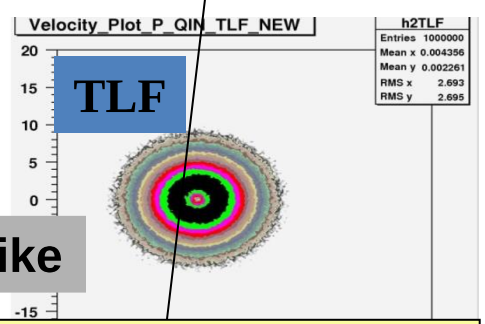

TLF

Evaporation-like

Sampling the Liquid – late emission

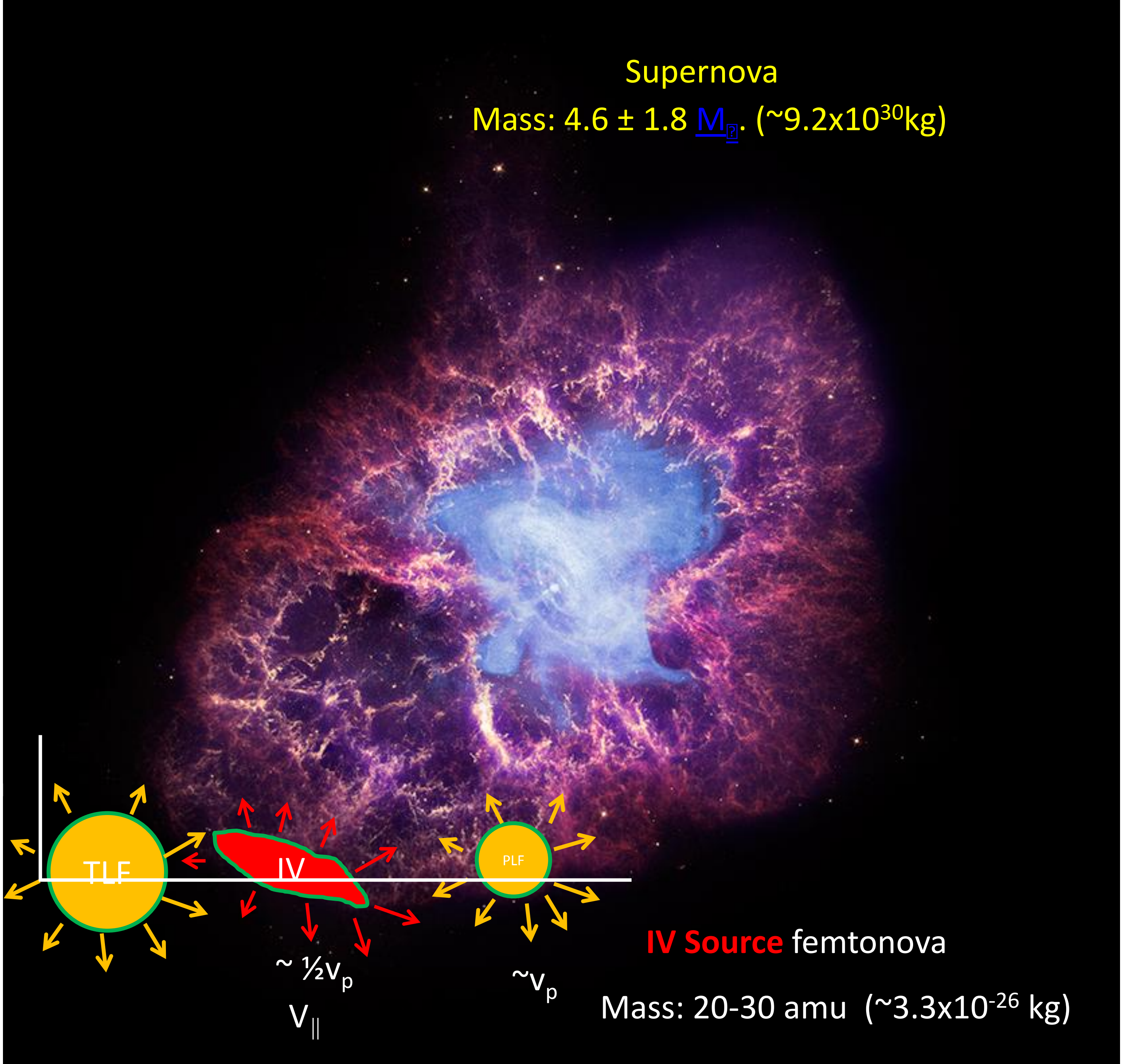

Supernova
Mass: 4.6 ± 1.8 M☉. (~9.2x10^30kg)
TLF
IV
PLF
~ ½v_p
V_||
~v_p
IV Source femtonova
Mass: 20-30 amu (~3.3x10^-26 kg)

Experiment Analysis

- 47 MeV/u Ar + ^{112,124}Sn
- Select the most violent collisions
- Identify the femtonova
  - Intermediate velocity source
    - nucleon-nucleon collisions early in the reaction
  - Choose light particles at 45 deg because moving source fits suggest that most products at that angle result from that source.
- Time scale from velocity of products from intermediate velocity source
- Temperature from Albergo model
- Density from Coalescense analysis

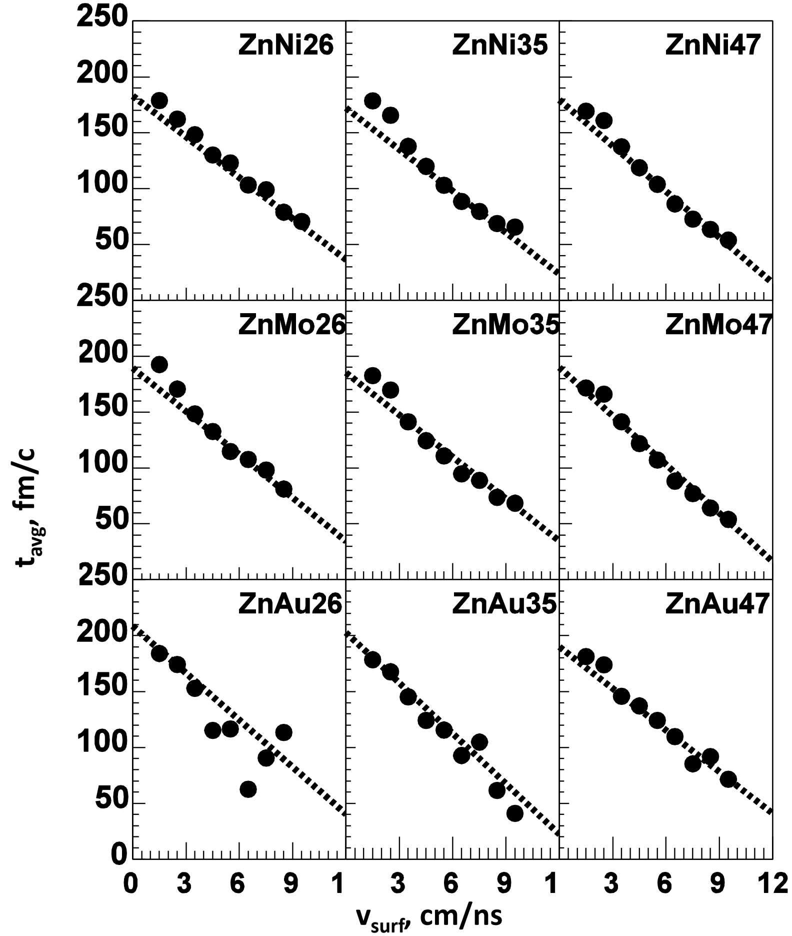

PRC **72** (2005) 024603
AMD MODEL CALCULATIONS
Proton Emission

NN Source Evolution- and properties

Coalescence Model Analysis

PHYSICAL REVIEW C VOLUME 24, NUMBER 1 JULY 1981

Precompound emission of light particles in the reaction $^{16}O + ^{238}U$ at 20 MeV/nucleon

T. C. Awes, G. Poggi,* and C. K. Gelbke
Cyclotron Laboratory, Michigan State University, East Lansing, Michigan 48824

B. B. Back and B. G. Glagola
Chemistry Division, Argonne National Laboratory, Argonne, Illinois 60439

H. Breuer and V. E. Viola, Jr.†
Departments of Physics and Chemistry, University of Maryland, College Park, Maryland 20742
(Received 8 December 1980)

$$\frac{d^2N(Z,N,E_A)}{dE_A d\Omega} = R_{np}^N \frac{A^{-1}}{N!Z!} \left(\frac{4\pi P_0^3}{3[2m^3(E-E_C)]^{1/2}} \right)^{A-1} \times \left(\frac{d^2N(1,0,E)}{dE\, d\Omega} \right)^A \quad (1)$$

where the double differential multiplicity for a cluster of mass number A containing Z protons and N neutrons and having a Coulomb-corrected energy E_A, is related to the proton double differential multiplicity at the same Coulomb corrected energy per nucleon, $E - E_C$, where E_C is the Coulomb barrier for proton emission. R_{np} is the neutron to proton ratio.

PHYSICAL REVIEW C VOLUME 17, NUMBER 3 MARCH 1978

Explosive nucleosynthesis, equilibrium thermodynamics, and relativistic heavy-ion collisions

A. Z. Mekjian
Nuclear Science Division, Lawrence Berkeley Laboratory, University of California, Berkeley, California 94720 and Department of Physics, Rutgers University, New Brunswick, New Jersey 08903

$$V = \frac{3h^3}{4\pi P_0^3} \left[(2s+1) \left(\frac{Z!N!A^3}{2^A} \right) e^{\frac{E_0}{T}} \right]^{\frac{1}{(A-1)}} \quad (2)$$

where h is Plancks constant and Z, N, and A are the same as in Eq. (1). E_0 is the binding energy, s the spin of the emitted cluster, and T is the temperature. Thus the radius, and therefore the volme, can be derived from the observed P_0 and temperature values assuming a spherical shape.

IL NUOVO CIMENTO VOL. 89 A, N. 1 1 Settembre 1985

Temperature and Free-Nucleon Densities of Nuclear Matter Exploding into Light Clusters in Heavy-Ion Collisions (*).

S. ALBERGO, S. COSTA, E. COSTANZO and A. RUBBINO
Dipartimento di Fisica dell'Università - Catania
Istituto Nazionale di Fisica Nucleare - Sezione di Catania
Centro Siciliano di Fisica Nucleare e di Struttura della Materia - Catania

$$T_{\mathrm{HHe}} = \frac{14.3}{\ln\left(\sqrt{9/8}(1.59\, R_{v_{\mathrm{surf}}})\right)}. \quad (1)$$

If Y represents a cluster yield, $R_{v_{\mathrm{surf}}} = Y(^2\mathrm{H})Y(^4\mathrm{He})/Y(^3\mathrm{H})Y(^3\mathrm{He})$ for clusters with the same surface velocity. The constants 14.3 and 1.59 reflect binding energy, spin, masses and mass differences of the ejectiles. Eq. (1) differs from the usual formulation only by the factor of $\sqrt{9/8}$ appearing in the logarithm term in the denominator.

Applied to ^{40}Ar + ^{112}Sn- NN Source

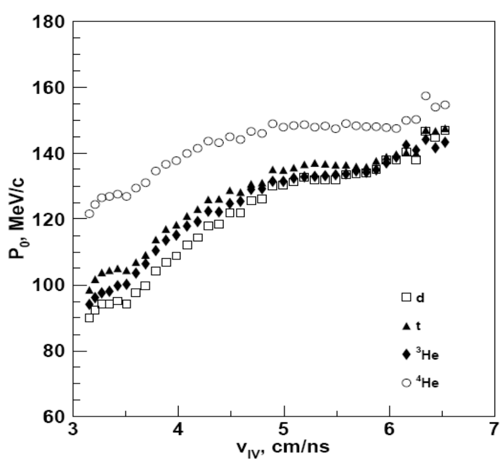

FIG. 1: Coalescence parameters, P_0 as a function of surface velocity in the intermediate velocity source frame. Reaction: 47 A MeV ^{40}Ar + ^{112}Sn

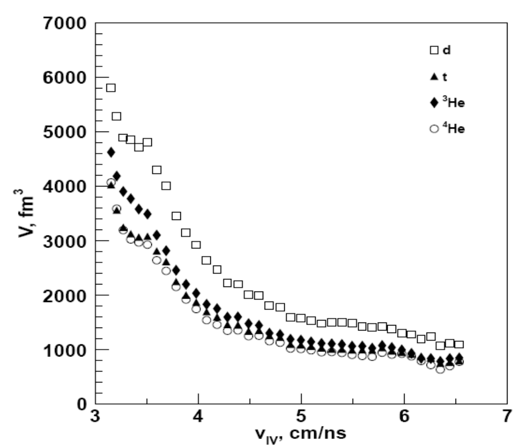

FIG. 2: Coalescence model volumes as a function of velocity in the intermediate velocity source frame. Reaction: 47 A MeV ^{40}Ar + ^{112}Sn

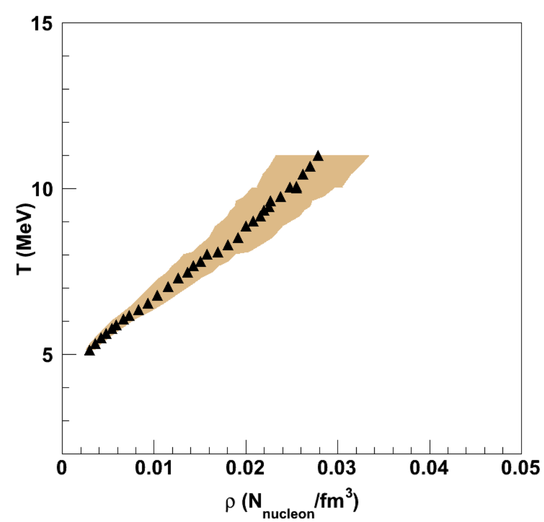

Temperatures and Densities

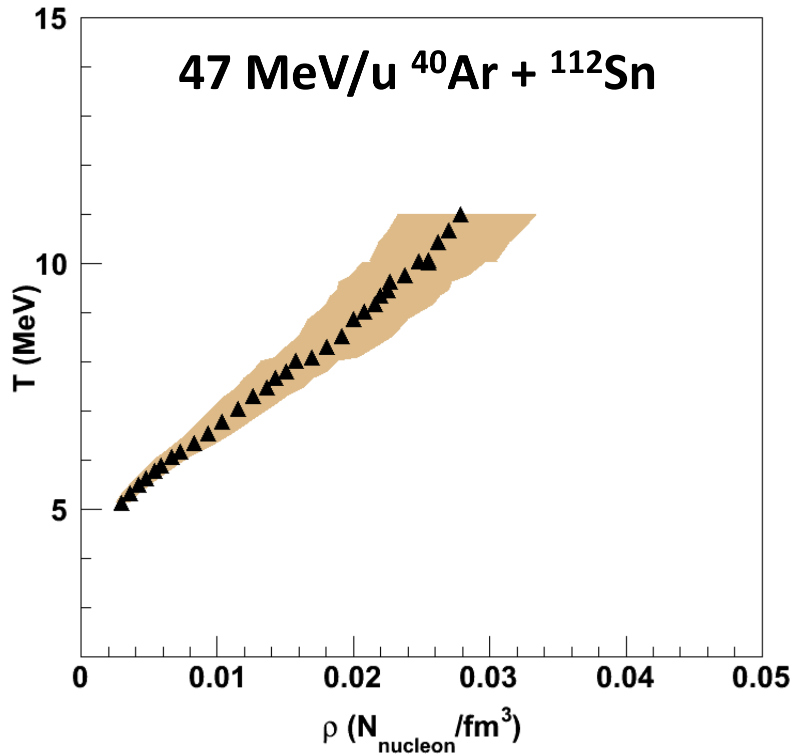

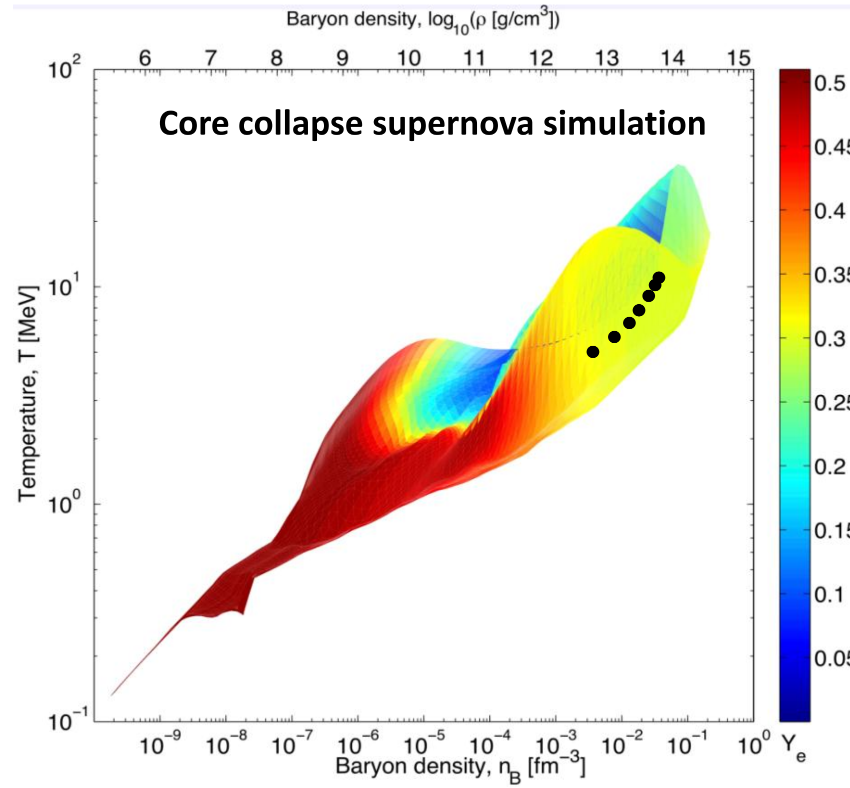

- Recall v_{surf} vs time calculation
- System starts hot
- As it cools, it expands

	Supernova	Heavy Ion Nuclear reaction
Density (nuc/fm³)	$10^{-10} < \rho < 2$	$2x10^{-3} < \rho < 3x10^{-2}$
Temperature (MeV)	~0 < T < 30	5 < T < 11
Electron fraction	$0 < Y_p < 0.6$	Y_p ~0.41

NSE calculation

Bonnet
Gulminelli

NSE

Yp=0.38?

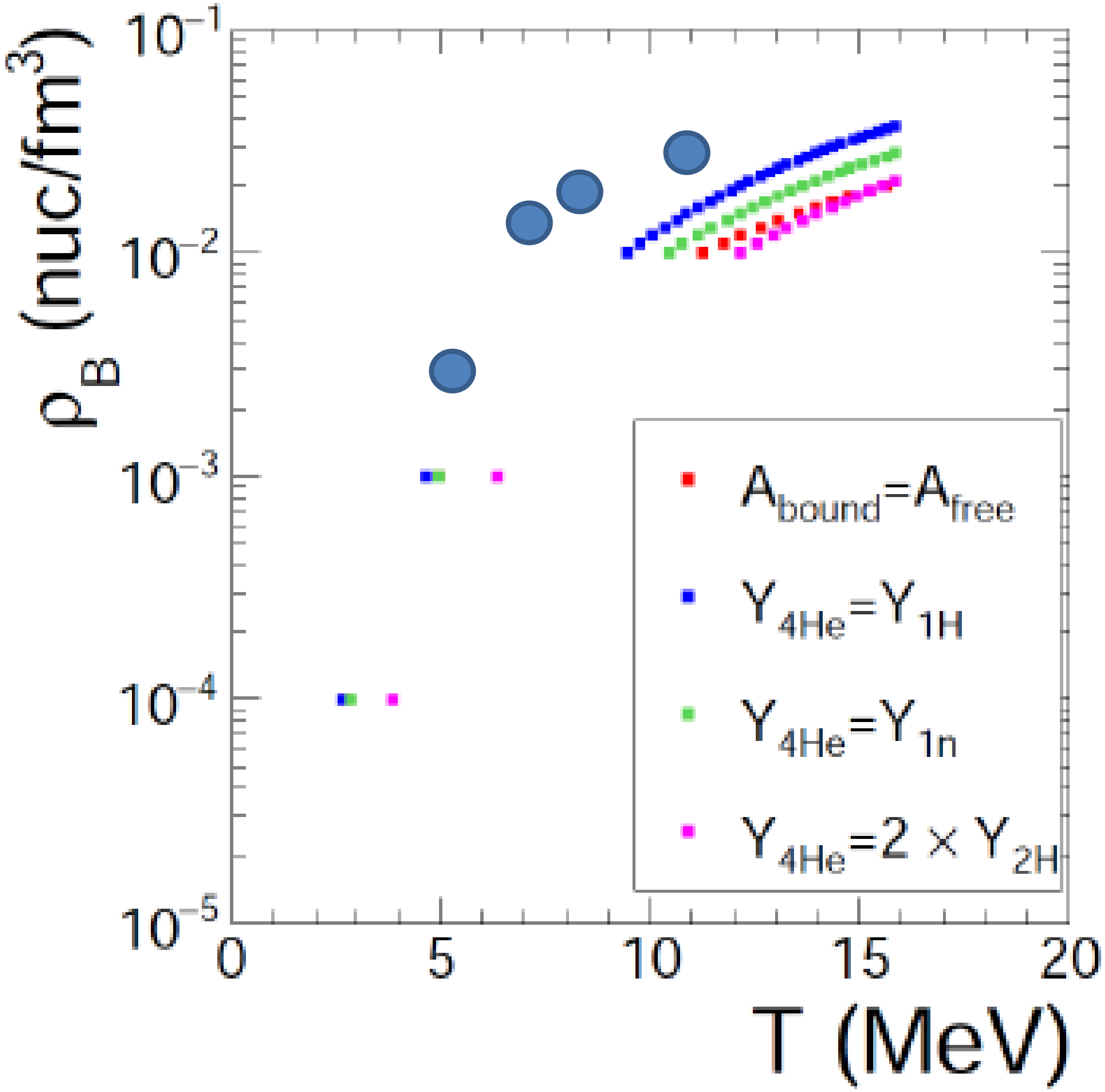

TAMU

Yp = 0.41

Neutrinos and gravitational attraction from Black Hole accretion disks

- O. L. Caballero *et al*.

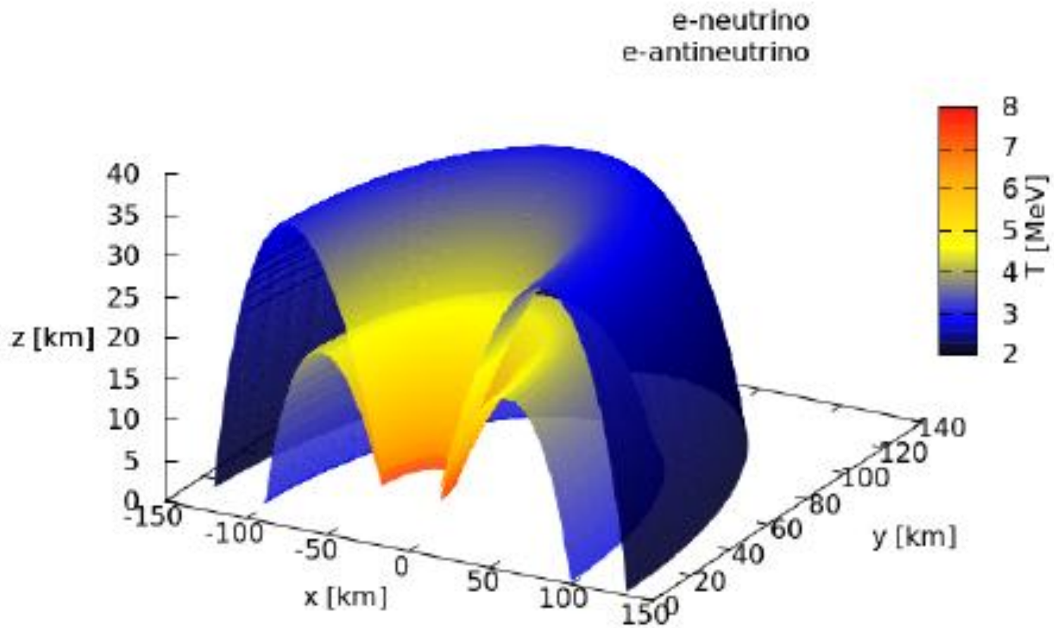

Figure 1. Electron neutrino (outter) and antineutrino (inner) surfaces corresponding to a snapshop at t=20 ms, of a hydrodynamical simulation of a torus around a 3 solar mass black hole.

PRL 108, 172701 (2012).

PRL **108**, 062702 (2012).

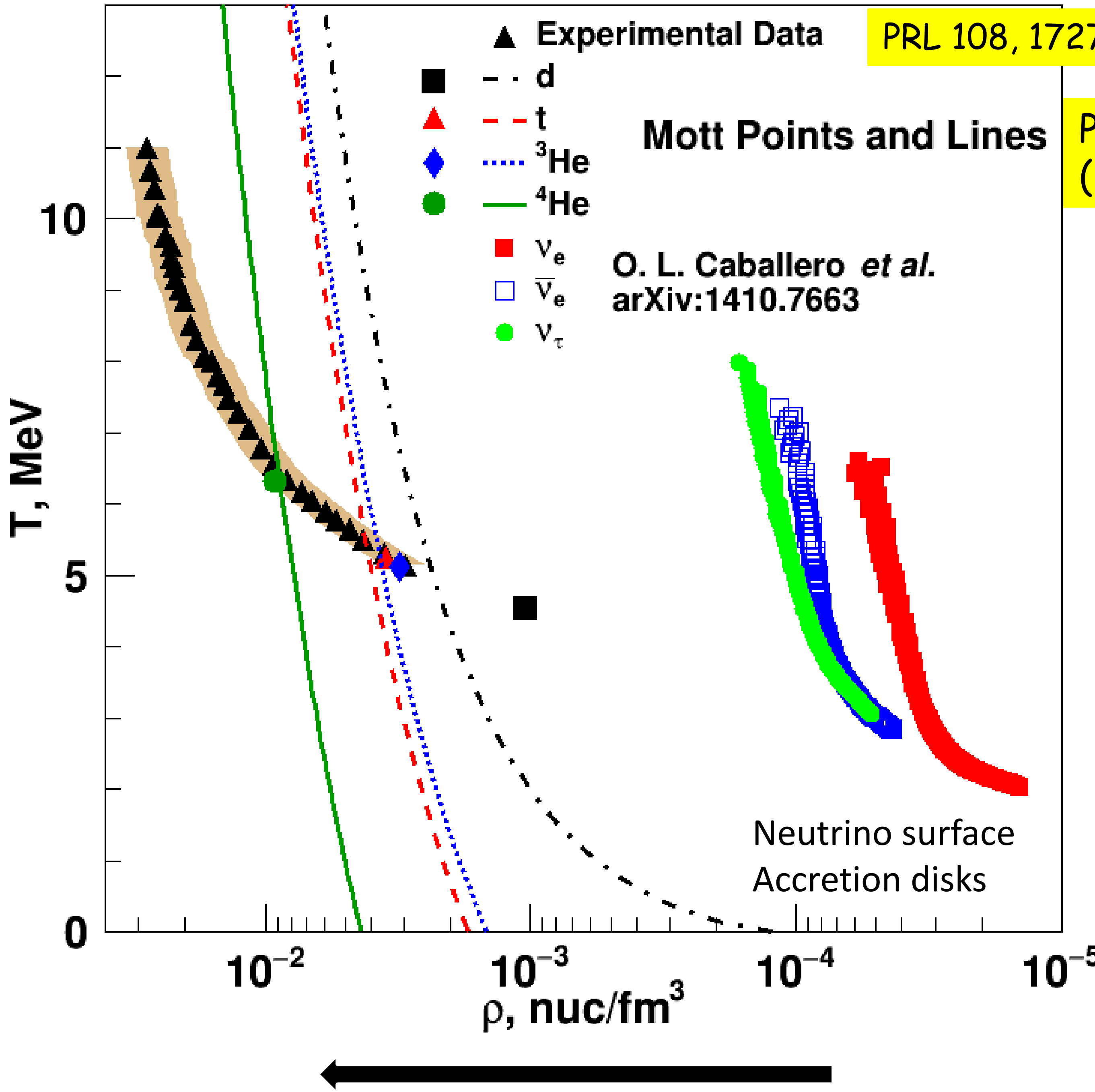

The Symmetry Energy Problem
Density Dependence ?

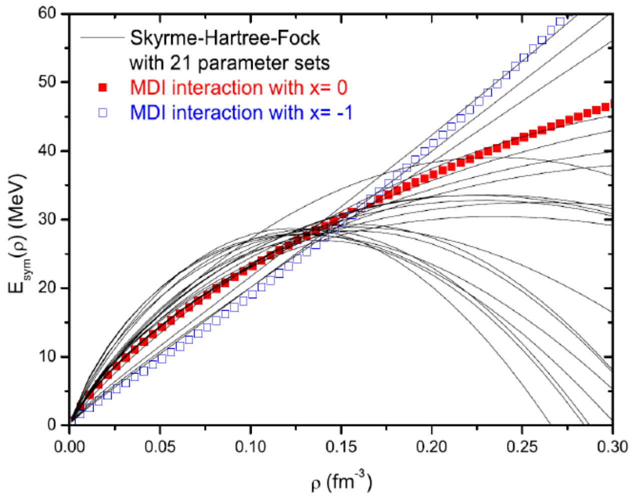

Experimentally or observationally constraining the density dependence of the symmetry energy over a broad range of densities is a complex problem-

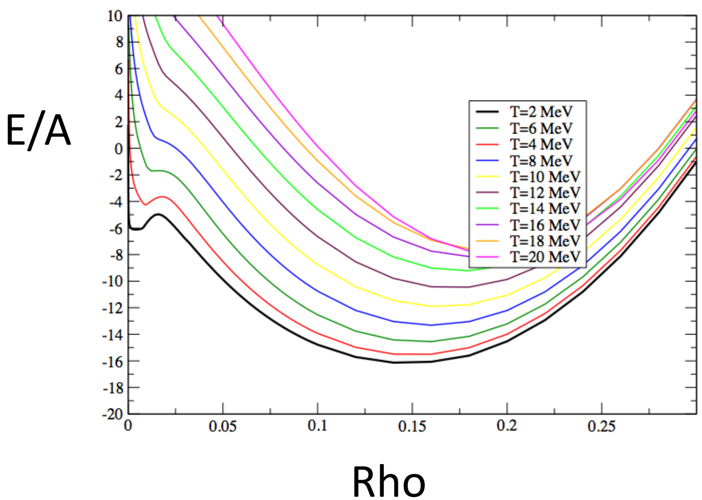

While low density situation would appear to be easier to constrain- cluster formation changes the medium This leads to additional complexity (opportunity)

Isoscaling Analysis and Symmetry Energy

isoscaling analysis. Such analyses have been reported in a number of recent papers [10, 11, 27, 28, 29, 30]. In this approach the yields of a particular species Y(N,Z) from two different equilibrated nuclear systems, 1 and 2, of similar temperature but different neutron to proton ratios, N/Z, are expected to be related through the isoscaling relationship

$$\frac{Y_2}{Y_1} = Ce^{((\mu_2(n)-\mu_1(n))N+(\mu_2(p)-\mu_1(p))Z)/T} \quad (2)$$

$$= Ce^{\alpha N+\beta Z} \quad (3)$$

where C is a constant and $\mu(n)$ and $\mu(p)$ are the neutron and proton chemical potentials.

The isoscaling parameters $\alpha = (\mu_2(n) - \mu_1(n))/T$ and $\beta = (\mu_2(p) - \mu_1(p))/T$, representing the difference in chemical potential between the two systems, may be extracted from suitable plots of yield ratios. Either parameter may then be related to the symmetry free energy, F_{sym}. With the usual convention that system 2 is richer in neutrons than system 1,

$$\alpha = 4F_{sym}((Z_1/A_1)^2 - (Z_2/A_2)^2)/T \quad (4)$$

$$\beta = 4F_{sym}((N_1/A_1)^2 - (N_2/A_2)^2)/T \quad (5)$$

where Z is the atomic number and A is the mass number of the emitter. Thus, F_{sym} may be derived directly from determinations of system temperatures, Z/A ratios, and isoscaling parameters. We emphasize that the present analysis is carried out for light species characteristic of the nuclear gas rather than, as in most previous analyses, for the intermediate mass fragments thought to be characteristic of the nuclear liquid.

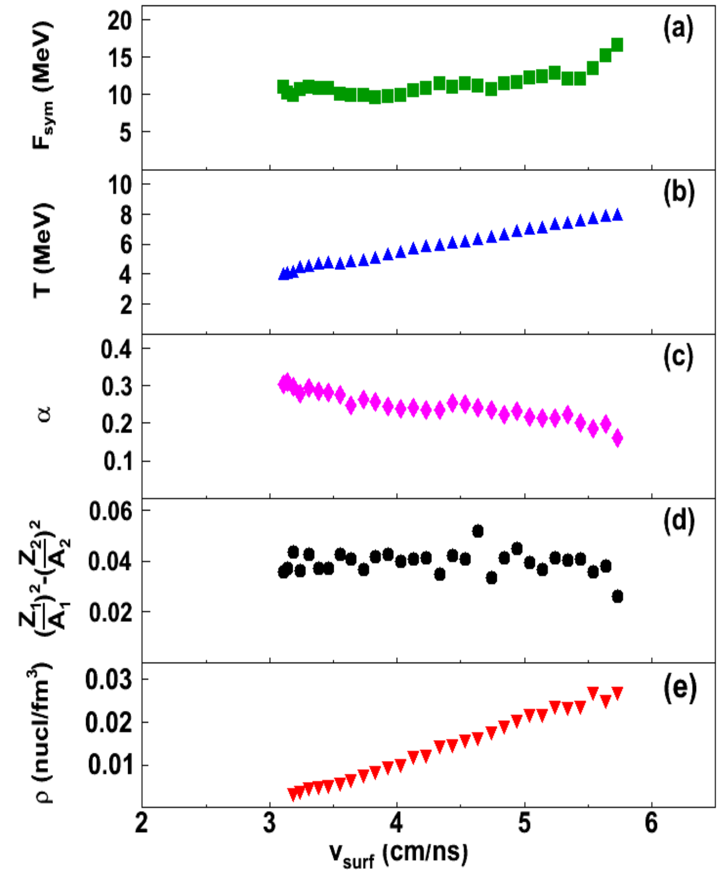

- **T, ρ increase with v_{surf}**
- **α extracted from light particle yields**
- **Decreases with v_{surf}**
- **F_{sym} Determined**

Symmetry Energy at Low Density

R. Wada et al.Phys. Rev. C 85, 064618 (2012)

At Low Density The Symmetry Energy is Determined by Cluster Formation. Analysis of Cluster Yield Ratios For Different N/Z Systems Allows Determination of The Symmetry Free Energy. Employment of Entropies Calculated with the QSM Model of Roepke, Typel et al (shown to be appropriate by other measured quantities) Allows Extraction of The LOW Density Symmetry Energy $F_{sym} + T \cdot S_{sym} = E_{sym}$

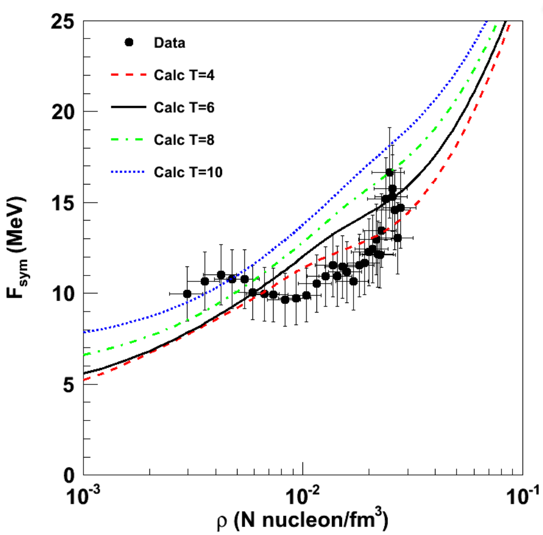

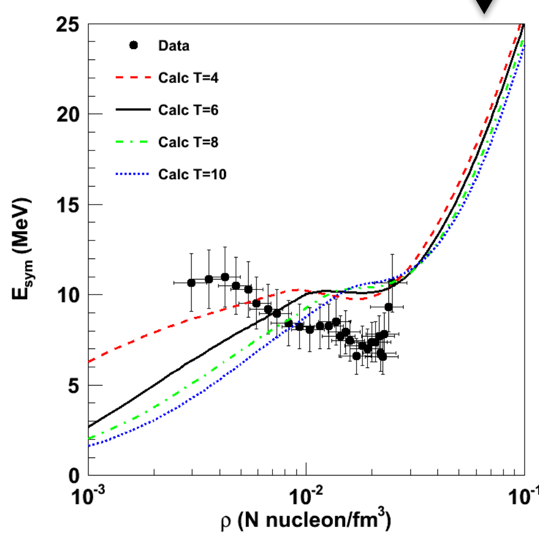

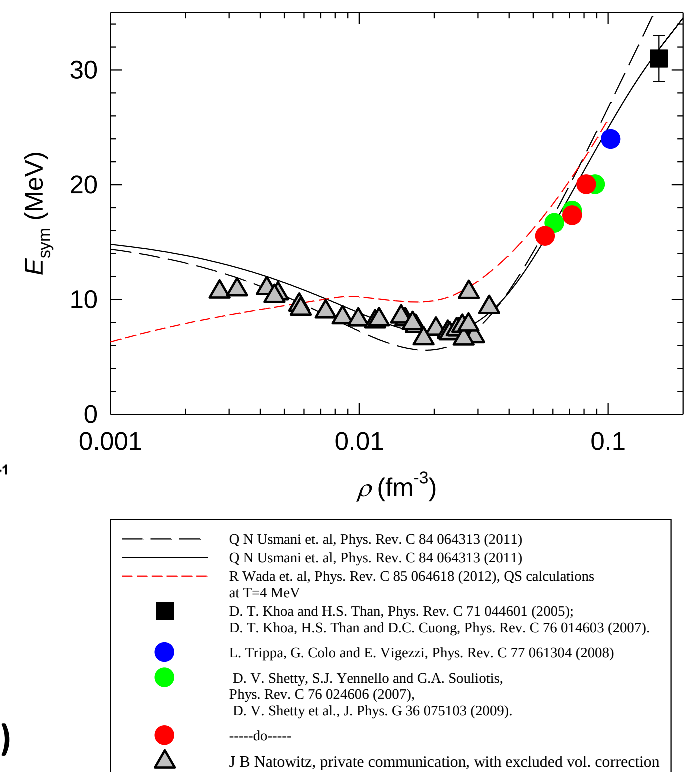

See Also

S. Typel *et al.*, Phys. Rev. C 81, 015803 (2010).

J.B. Natowitz et al., Phys.Rev.Lett.104:202501 (2010).

S. Kowalski et al. Phys. Rev. C. 74 014601 (2007)

K. Hage;, J.B. Natowitz and G. Roepke arXiv:1401.2074 (2014)

Symmetry energy: low density limit

At Low Density The Symmetry Energy is Determined by Cluster Formation. Analysis of Cluster Yield Ratios For Different N/Z Systems Allows Determination of The Symmetry Free Energy. Employment of Entropies Calculated with the QSM Model of Roepke, Typel et al (shown to be appropriate by other measured quantities) Allows Extraction of The LOW Density Symmetry Energy $F_{sym} + T\cdot S_{sym} = E_{sym}$

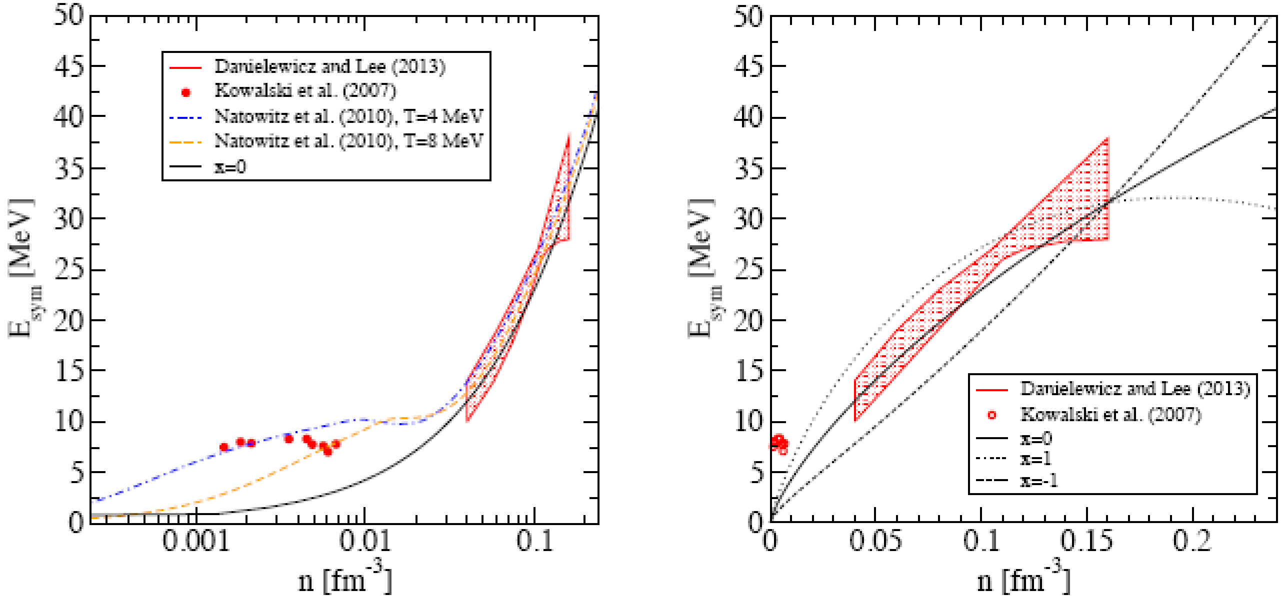

<u>The equation of state and symmetry energy of low density nuclear matter</u>

K. Hagel, G. Roepke and J. Natowitz , EPJA, **50**, 39 (2014)

See also

S. Typel *et al*., Phys. Rev. C 81, 015803 (2010).

J.B. Natowitz et al., Phys.Rev.Lett.104:202501 (2010).

Clustering in Low Density Nuclear Matter

Alpha Mass Fractions

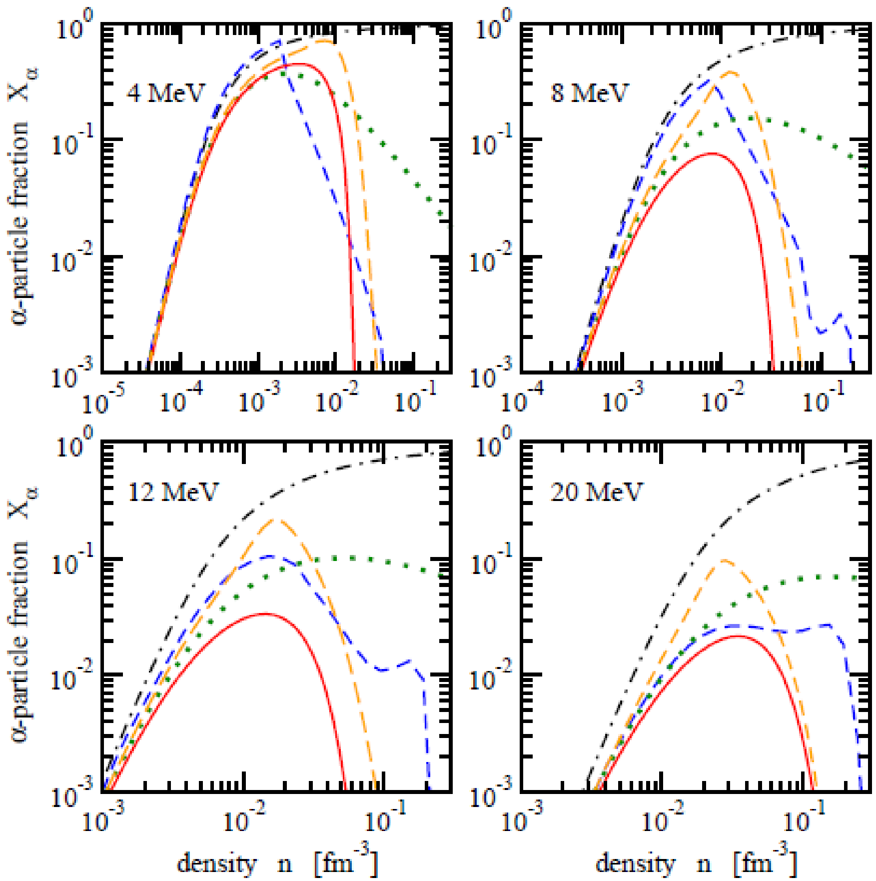

FIG. 15: (Color online) Comparison of α-particle fractions in symmetric nuclear matter as a function of the density at four temperatures for the virial expansion (black dashed-dotted lines), NSE (green dotted lines), the EoS of Shen et al. [29] (blue dashed lines), the generalized RMF model (red solid lines) and the QS approach (orange dashed lines). Note the different scales on the x-axes.

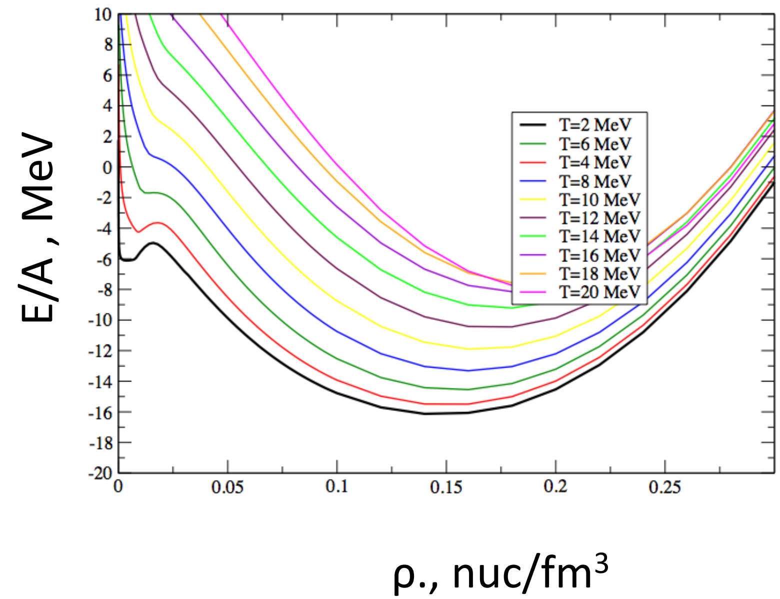

S. Typel, G. Roepke, T. Klahn D. Blashke and H.H. Wolter ArXiv 0908.2344v1 August 2009

CYCLOTRON INSTITUTE
Texas A&M University

Test of Astrophysical Equations of State Equilibrium Constant, K_α

- Many tests of EOS are done using mass fractions. Various calculations include various different competing species., if all relevant species are not included, mass fractions are not accurate.

- Equilibrium constants, e.g.,

should be independent of proton fraction and choice of competing species.

- Models converge at lowest densities, but many are significantly above data at higher density

- Lattimer & Swesty with K=180, 220 show reasonable agreement with data

- QSM with in-medium binding energy shifts works well

L. Qin et al.PRL **108** 172701 (2012).

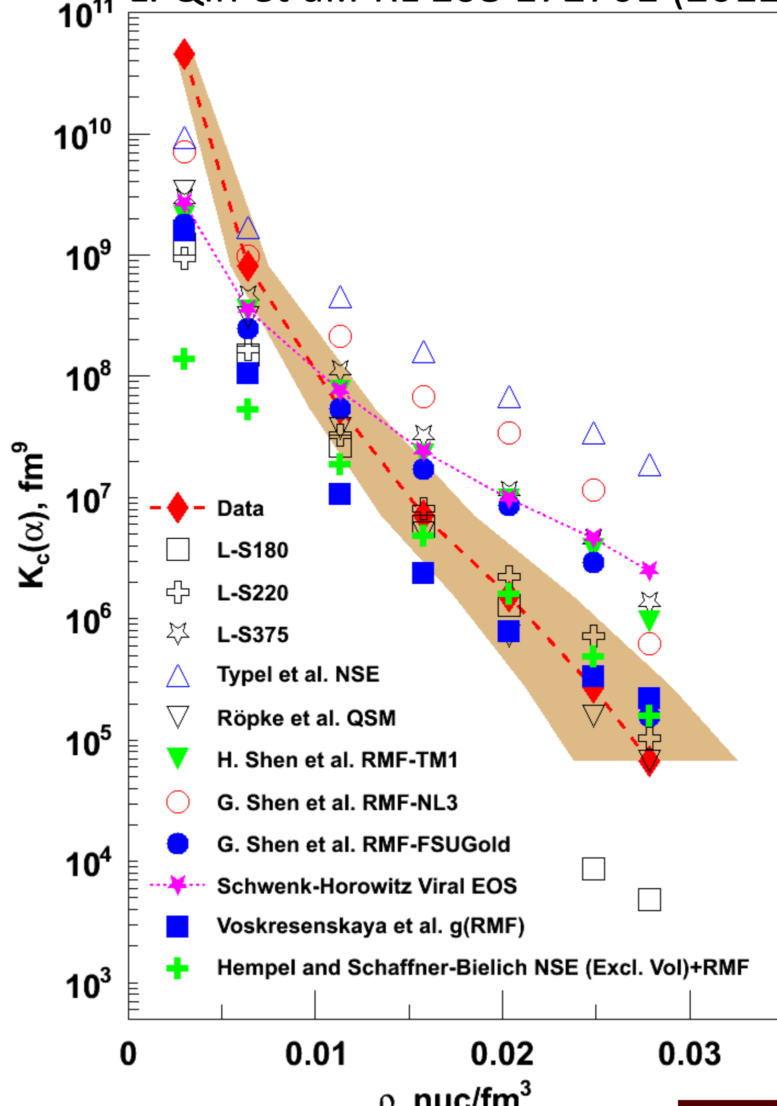

From Wikipedia, the free encyclopedia

The **equilibrium constant** of a chemical reaction

$$\alpha A + \beta B ... \rightleftharpoons \rho R + \sigma S ...$$

is the value of the reaction quotient when the reaction has reached equilibrium.

For a general chemical equilibriumthe thermodynamic equilibrium constant can be defined such that, at equilibrium,[1][2]

$$K^{\ominus} = \frac{\{R\}^{\rho}\{S\}^{\sigma}...}{\{A\}^{\alpha}\{B\}^{\beta}...}$$

where curly brackets denote the thermodynamic activities** of the chemical species. The right-hand side of this equation corresponds to the reaction quotient Q for arbitrary values of the activities. The reaction coefficient becomes the equilibrium constant as shown when the reaction reaches equilibrium.

An equilibrium constant value is independent of the analytical concentrations of the reactant and product species in a mixture, but depends on temperature and on ionic strength. Known equilibrium constant values can be used to determine the composition of a system at equilibrium.

The equilibrium constant is related to the standard Gibbs free energy change for the reaction.

$$\Delta G^{\ominus} = -RT \ln K^{\ominus}$$

If deviations from ideal behavior are neglected, the activities of solutes may be replaced by concentrations, [*A*], and the activity quotient becomes a concentration quotient, K_c.

$$K_c = \frac{[R]^{\rho}[S]^{\sigma}...}{[A]^{\alpha}[B]^{\beta}...}$$

K_c is defined in an equivalent way to the thermodynamic equilibrium constant but with concentrations of reactants and products instead of activities. (K_c appears here to have units of concentration raised to some power while K is dimensionless; however the concentration factors in K_c are properly divided by a standard concentration so that K_c is dimensionless also.

Assuming ideal behavior, the activity of a solvent may be replaced by its mole fraction, (approximately by 1 in dilute solution). The activity of a pure liquid or solid phase is exactly 1. The activity of a species in an ideal gas phase may be replaced by its partial pressure.

** In chemical thermodynamics, **activity**) is a measure of the "effective concentration" of a species in a mixture. The species' chemical potential depends on the activity Activity depends on temperature, pressure and composition of the mixture, among other things. The difference between activity and other measures of composition arises because molecules in non-ideal gases or solutions interact with each other, either to attract or to repel each other.

Equilibrium constants from α-particles --model predictions

( ) ______

- Many tests of EOS are done using mass fractions and various calculations include various different competing species.
- If any relevant species are not included, mass fractions are not accurate.
- Equilibrium constants should be more robust with respect to the choice of competing species assumed in a particular model if interactions are the same
- Differences in the equilibrium constants may offer the possibility to study the interactions
- Models converge at lowest densities, but are significantly below data

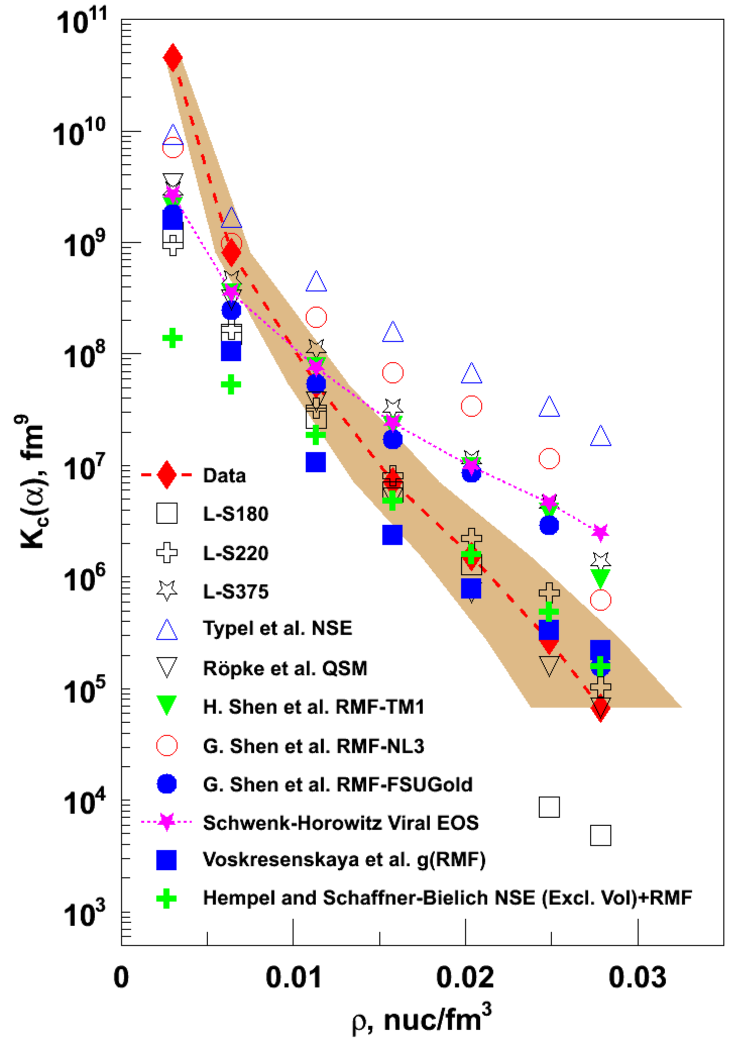

PRL **108** (2012) 172701.

Constraining supernova equations of state with equilibrium constants from heavy-ion collisions

Matthias Hempel*
Department of Physics, University of Basel, Klingelbergstrasse 82, 4056 Basel, Switzerland

Joseph Natowitz, Kris Hagel, Stefan Typel, and Gerd Röpke (preliminary author list)
(Dated: January 29, 2015)

- Phys. Rev. C **91**, 045805 (2015).
- Dependence of Equilibrium constants on various quantities
  - Asymmetry of system
  - Coulomb effects
  - Particle degrees of freedom
- Include comparison where possible to other particle types observed in experiment (d, t, ^{3}He)
- Other EOS models

Constraining the EOS

- STOS
  - Treats only n, p, α
  - Fits $K_{eq}(\alpha)$ with heavy nuclei suppression, but cannot fit d, t, ^{3}He

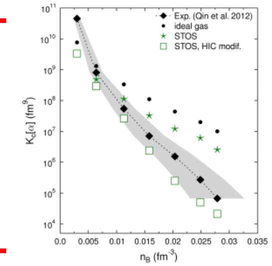

- LS
  - Treats n, p, α and heavy nuclei
  - Fits $K_{eq}(\alpha)$ in unmodified form, but not when heavy nuclei suppressed

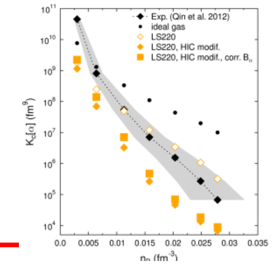

- NL3, FSUgold
  - Uses different assumptions in different density regimes
    - Large rho: uniform nuclear matter of nucleons
    - Intermediate rho: RMF with Hartree calculations leading to nucleons and heavy nuclei
    - Small rho: viral EOS to second order

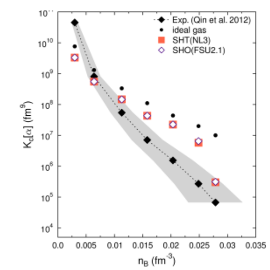

- gRDF
  - Treats nucleons, light and heavy nuclei
  - Interaction is meson-exchange based relativistic mean field approach.

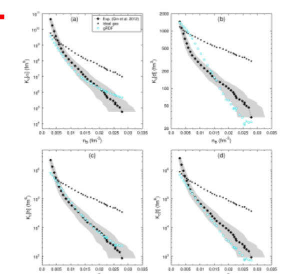

- QS
  - Microscopic treatment with systematic quantum statistical approach
  - Effects of medium on cluster are taken into account.

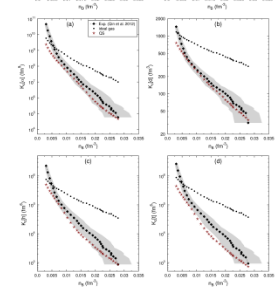

Test Coulomb effects

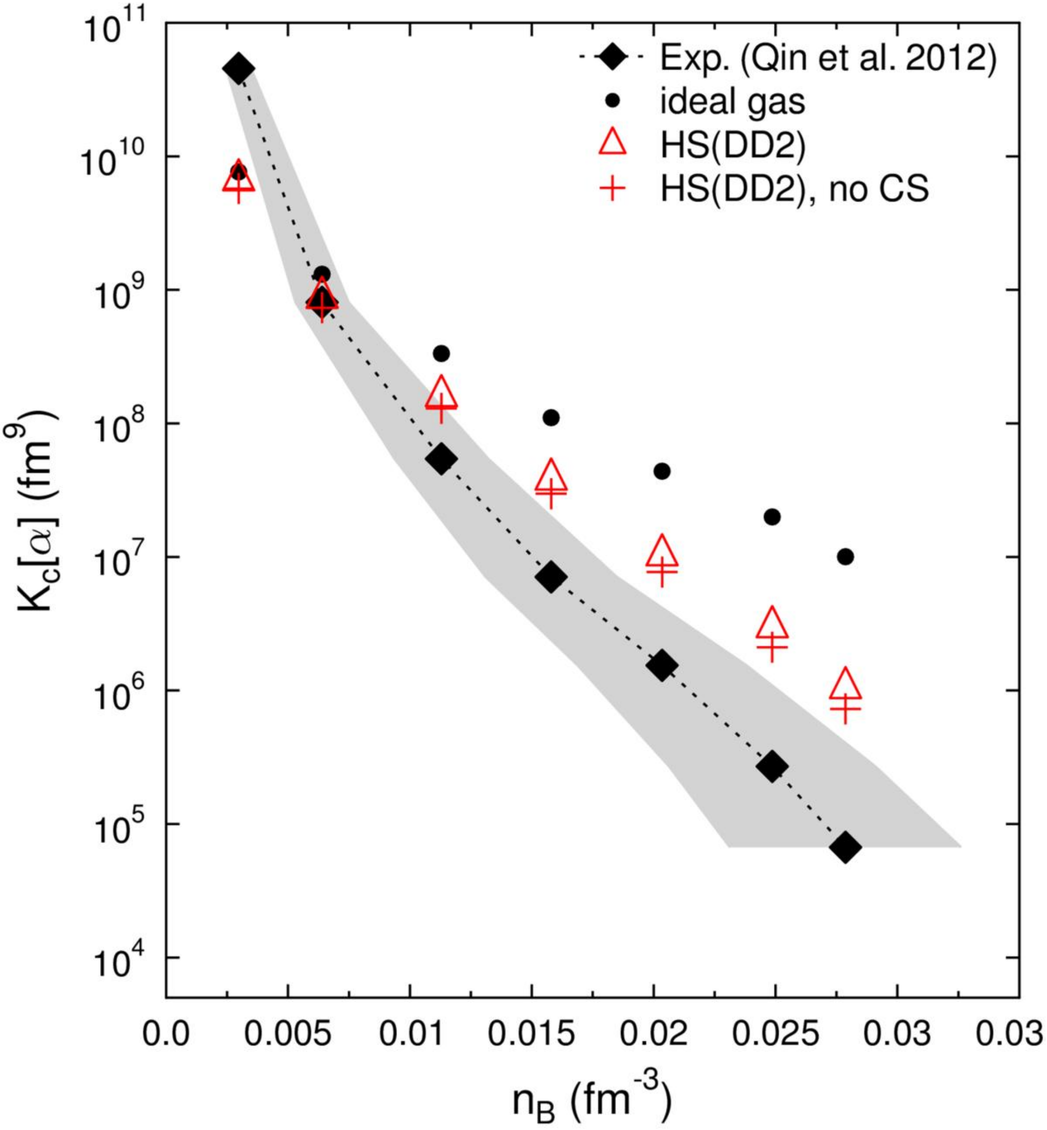

- In SN matter, coulomb interactions screened by surrounding electrons in contrast to matter in heavy ion collisions
- Small effect in calculations when screening is turned off.

Composition

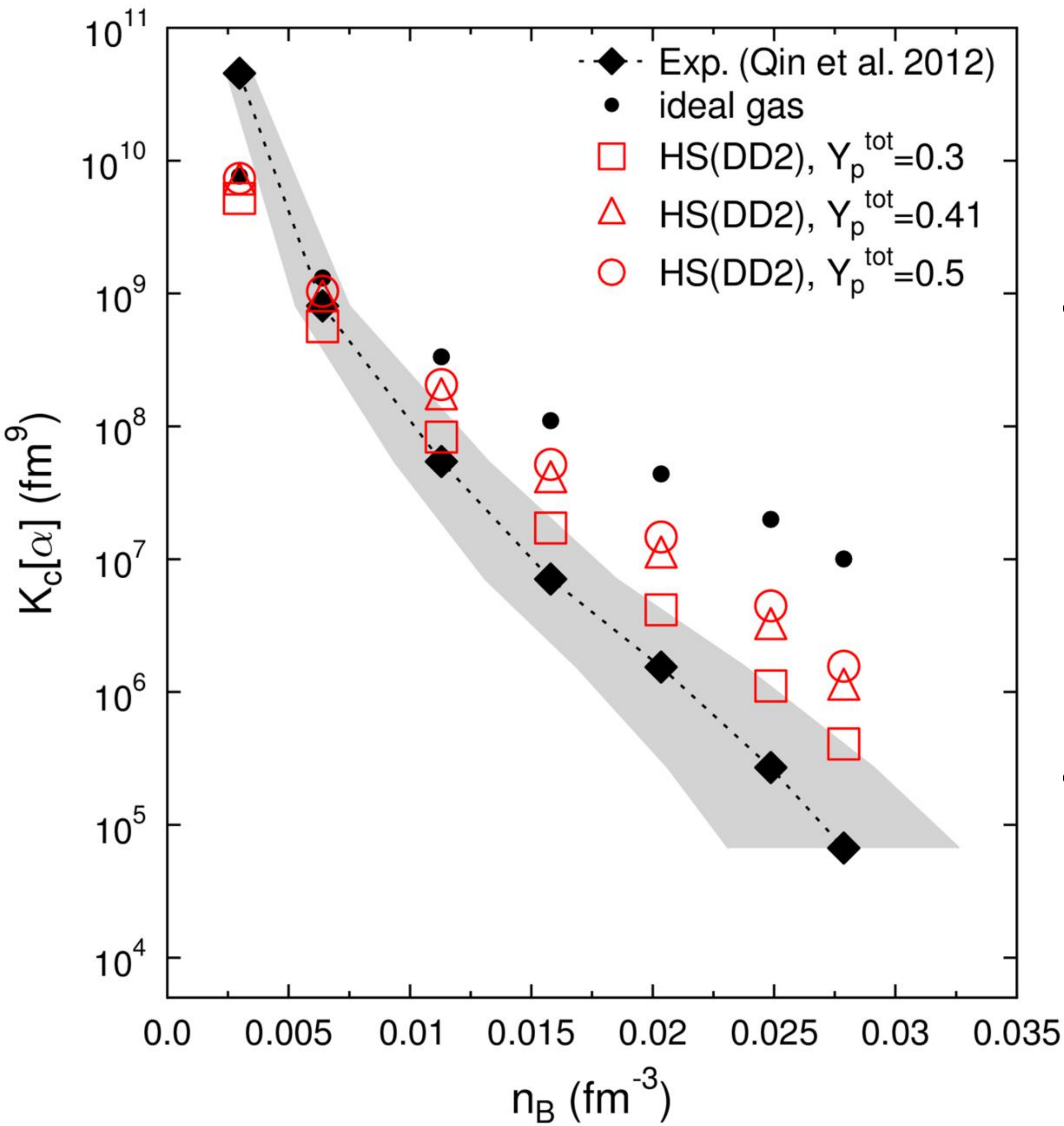

- Ideal gas
  - Chemical potentials cancel in the case of equilibrium
  - Function of temperature only.
  - no ρ or Y_p dependence.
- When interaction is present
  - Composition dependent
  - Values converge to ideal gas at low densities
  - Increase in K_{eq} with increasing Y_p at as density increases.
- Use Y_p = 0.41 in remainder of calculations since that is what was extracted from experiment.

Constraining supernova equations of state with equilibrium constants from heavy-ion collisions

Matthias Hempel, Kris Hagel, Joseph Natowitz, Gerd Röpke, Stefan Typel Phys. Rev. C 91, 045805 (2015)

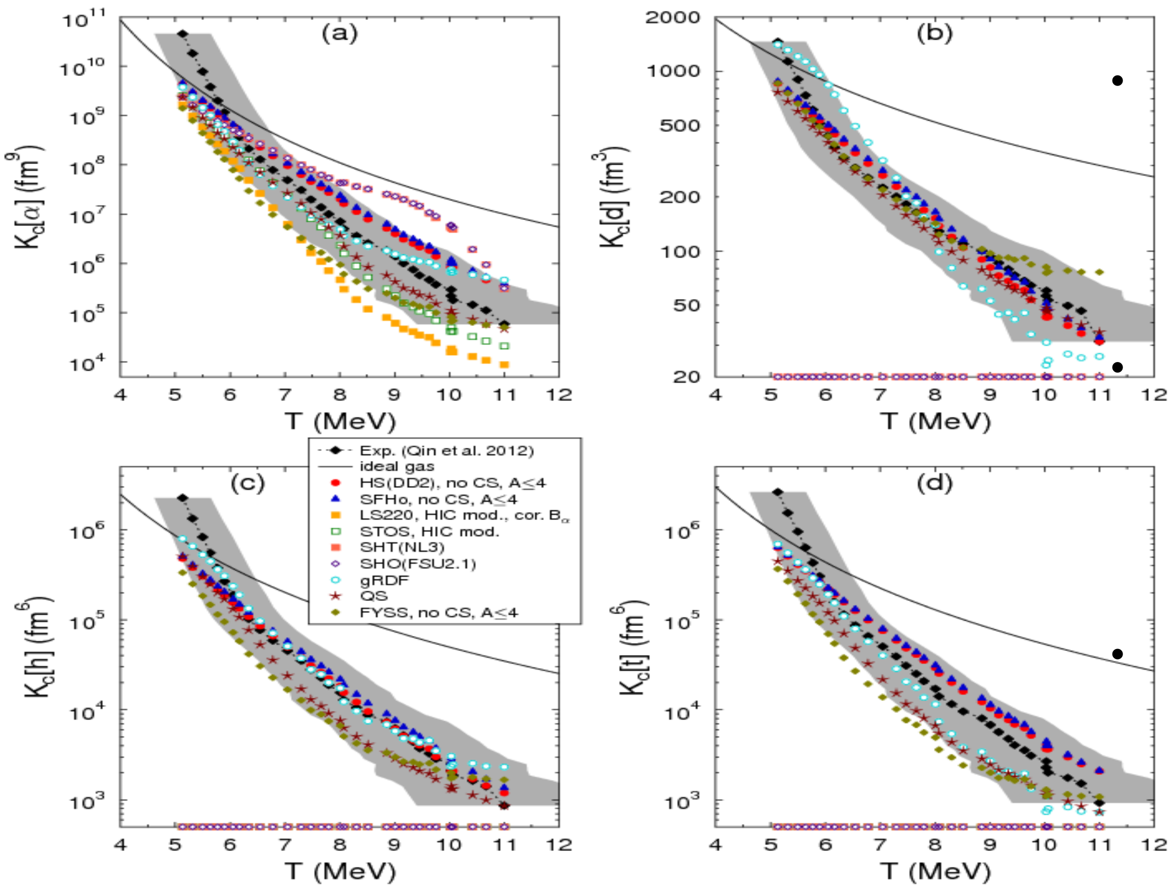

- Two groups of calculations
  - n, p, α calculations which predict $K_{eq}(\alpha)$, but cannot predict other species.
  - Models with n, p, d, t, ^{3}He, α
- Low densities
  - All $K_{eq}(\alpha)$ converge to ideal gas
  - But are below experimental data which result from the very late stages of the reaction
- Models that treat all light particles are generally within error bars

Figure 2. Equilibrium constants vs temperature. This figure shows the main results of our investigation: EC for (a) alpha particles, (b) deuterons,(c) helions, and (d) tritons as a function of temperature. The grey band represents the experimental uncertainty for the temperature determinations. Experimental data (black diamonds) is compared with various different theoretical models, which are all adapted for the conditions in HIC, as far as possible. The ECs of nuclei which are not included in a model are put on the x-axis. The black lines show the ECs of the ideal gas model, which are solely a function of temperature.

QUESTIONS

- Cluster Production
- Fragment angular momenta
- Gas vs Liquid
- Early Recognition, MST, Simulated Annealing
- Shell Effects
- Short Range Correlations
- Use of Hybrid Models

Collaborators

M. Hempel, K. Hagel, S. Kowalski, R. Wada, L. Qin,J. B. Natowitz, G. Röpke, S. Typel, M. Barbui, K. Schmidt, S. Wuenschel, E. J. Kim, G. Giuliani, S. Shlomo, A. Bonasera, Z. Chen, M. Huang, J. Wang, H. Zheng, M. R. D. Rodrigues, D. Fabris, M. Lunardon, S. Moretto, G. Nebbia, S. Pesente, V. Rizzi, G. Viesti, M. Cinausero, G. Prete, T. Keutgen, Y. El Masri, Z. Majka, and Y. G. Ma

Texas A&M University, College Station, Texas
INFN Laboratori Nazionali di Legnaro, Legnaro, Italy
INFN Dipartimento di Fisica, Padova, Italy
Jagellonian University, Krakow, Poland
Silesian University, Katowice, Poland
University of Rostock, Rostock, Germany
Basel University, Basel, Switzerland
UCL, Louvain-la-Neuve, Belgium
Shanghai Institute of Nuclear and Applied Physics, Shanghai, China